J. Membrane Biol. 152, 25–37 (1996)

The Journal of
Membrane
Biology

Cultured Giant Fiber Lobe of Squid Expresses Three Distinct Potassium Channel Activities in Selective Combinations

W.-S.D. Griggs[*,2], **Y. Hanyu**[1,2], **G. Matsumoto**[2]
[1]PRESTO, Research Development Corporation of Japan, [2]Supermolecular Division, Electrotechnical Laboratory, Tsukuba, Ibaraki 305, Japan

Received: 24 October 1995/Revised: 5 March 1996

Abstract. Neurons from the giant fiber lobe (GFL) of squid *Loligo bleekeri* were dissociated and cultured. The ionic currents were recorded using whole-cell patch clamp methods. The sodium current and the noninactivating potassium current like those elicited by the giant axon were among the currents expressed in axonal bulbs and bulblike structures upon dissociation. Meanwhile axonless cell bodies did not elicit such currents. Axonless cell bodies and some bulblike structures elicited two kinds of inactivating potassium currents, the slow- and the fast-inactivating current, which differed in their inactivation kinetics and pharmacology. Within 24 hr of plating, the current composition remained the same. While the noninactivating current was not sensitive to 4-aminopyridine, the two inactivating currents were sensitive, the slow-inactivating current being more sensitive. Selective combinations of the sodium current and the three potassium currents expressed in different structures of the acutely dissociated GFL could have resulted from cellular control of synthesis and transportation of the channel proteins to the somatic and the axonal membrane. The sodium current and the noninactivating potassium current could be recorded from some axonless cell bodies maintained in culture for over three days, indicating that the separation of the giant axon from its somata could result in the transportation of the channels normally expressed on the giant axon membrane to the somatic membrane.

Key words: Squid — Giant fiber lobe — Potassium current — Inactivation kinetics — 4-aminopyridine — Channel expression

Introduction

Potassium channels have the greatest degree of diversity among ion channels. Different types of potassium channels can be found in the same cell, and different cells can exhibit similar types of potassium channels. Therefore, this diversity can not be accounted for simply by cell type (for review, *see* [28]). Different potassium channels could stem from different genes, while alternative splicing of the genes also contributes to the diversity (for review, *see* [27]). In addition to what is provided by the potassium channels encoded in the genome, other factors have also been proposed as enhancing this diversity such as different levels of expression of a single mRNA [16] and heteromultimeric assembly of the subunits [4, 17, 18, 24, 29]. Cytoskeleton-destructing agents have also been found to affect the inactivation characteristics of the potassium currents [20, 21, 22, 23]. The diverse functions that neurons serve require the availability of channels with diverse properties as well as the regulation of synthesis, transport and distribution of these channels.

The giant axon of squid is formed by fusion of axons from hundreds of cell bodies residing in the giant fiber lobe (GFL) of the stellate ganglion. It is generally believed that cell bodies in the giant fiber lobe of squid are the sites where proteins including ion channels are synthesized and packaged. It is also believed that the giant axon serves as a destination for a subset of these channels.

Upon dissociation of the GFL cells, structures with different morphology can be observed as shown in Fig. 1. Axonless cell bodies (cell bodies without processes, marked as CB) had diameters of 25–50 μm which did not change obviously in culture. Some cells retained part of their axons (marked as AX). The length of the axons varied from cell to cell and remained the same in culture. Lengths from 10 to 200 μm have been observed. The

Present address: Department of Physiology, School of Medicine, Johns Hopkins University, Baltimore, MD 21205.

Correspondence to: Y. Hanyu

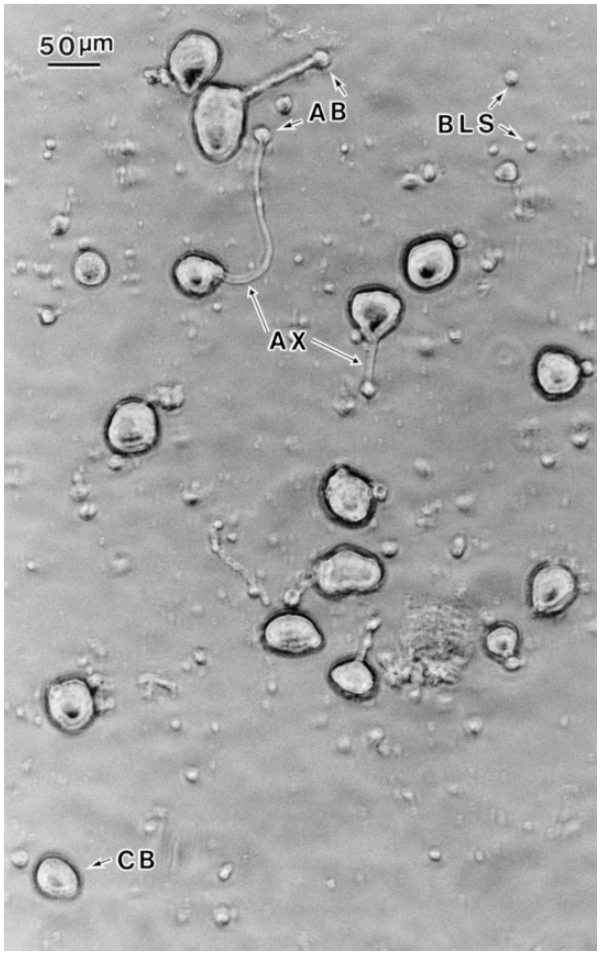

Fig. 1. GFL, axonless cell bodies, axonal bulbs and bulblike structures. The picture was taken a few hours after plating. The axonless cell bodies (marked CB) had diameters ranging between 25 and 50 μm. Some cells retained their axons (marked AX) whose lengths ranged 10 to 200 μm. The axonal bulbs (marked AB) at the end of the axons had diameters about 10 μm. The bulblike structures (marked BLS) had diameters about 10–15 μm.

end of the axon sealed to form an axonal bulb (marked as AB) [9]. The axonal bulbs were usually round with diameters about 10 μm and grew in size in culture. Isolated bulblike structures (marked as BLS) were also present particularly on day 0 and day 1. These structures usually had diameters of 10–15 μm. They were probably dissociated axonal bulbs or were formed from fragments of axons during preparation. The membrane of axonal bulbs and that of bulblike structures represents the membrane in between the giant axon and its cell bodies.

We report here characterization of the ionic currents in GFL of *L. bleekeri*. In contrast to the case of giant axon where a delayed rectifying current is the only potassium current elicited, three kinds of potassium currents were recorded from GFL. These three potassium currents, namely, noninactivating, slow- and fast-inactivating potassium currents, were distinct in their biophysical and pharmacological characteristics. These potassium currents, together with the sodium current, were present in different combinations in different structures of the GFL. The currents form a gradient along the transportation pathway from soma to axon, with slow-inactivating potassium current elicited in both the somatic and proximal axonal membrane, and sodium and noninactivating potassium current elicited in all the axonal membrane. The current components elicited by the axonless cell bodies could vary after the cells had been maintained in primary culture for a few days.

Some of the results reported here have been presented in abstract form [10].

Materials and Methods

Cell Culture

GFL of the stellate ganglion of squid (*L. bleekeri*) was dissected and the cell bodies were dissociated and cultured in a manner similar to [9, 19]. The dissection was carried out in circulating oxygenated artificial sea water (8°C). After dissection, GFLs were treated with nonspecific protease (5–10 mg/ml, type XIV, Sigma) for 1–1.5 hours at room temperature. The protease was dissolved in ASW, which consisted of (in mM): 440 NaCl, 5 KCl, 10 $CaCl_2$, 50 $MgCl_2$, 10 HEPES (pH 7.8), and supplemented with 50 U/ml penicillin G and 0.5 mg/ml streptomycin. After being rinsed in ASW three times, GFLs were transferred to petri dishes containing culture medium. The culture medium was consisted of Leibovitz's L-15 tissue culture medium (Gibco) and the following salts to match those in the sea water (in mM): 263 NaCl, 4.64 KCl, 9.05 $CaCl_2$, 49.54 $MgCl_2$ [2, 8, 9]. The culture medium was also supplemented by 2 mM L-glutamine, 2 mM HEPES (pH 7.8), 50 U/ml penicillin G, 0.5 mg/ml streptomycin and 6% fetal bovine serum (Gibco). When only the part of GFL which gave rise to the last giant axon was dissected, the results obtained were not different from those obtained when a larger portion of GFL was dissected.

The glass coverslips were washed in acetone and ethanol for 20 min each with sonication. After being coated with 10% Concanavalin A (Sigma) in distilled water for 20–40 min, the coverslips were washed four times with distilled water and were then left to dry under UV light for 20 min.

Cells were dissociated by pipetting 30–50 times in 400 μl culture medium per GFL in an Eppendorf tube, with a pasteur pipette coated with silicon (Sigmacote, Sigma). Then the medium containing the dissociated cells was transferred onto glass coverslips placed in 35 mm petri dishes. The dishes were left undisturbed under room temperature for 1 hr before 2 ml medium was added and the dishes were then placed in incubator set at 15.5°C. The medium was changed every three days. Cells could be kept in culture for at least two weeks.

Electrophysiological Measurements

Whole-cell patch-clamp techniques were employed to record the ionic currents from the axonless cell bodies, the axonal bulbs and the bulblike structures (*see* Results). Prior to recording from the axonal bulb, the axon connecting the axonal bulb and its soma was cut with a tungsten wire [9]. All experiments were performed at 17°C. The ex-

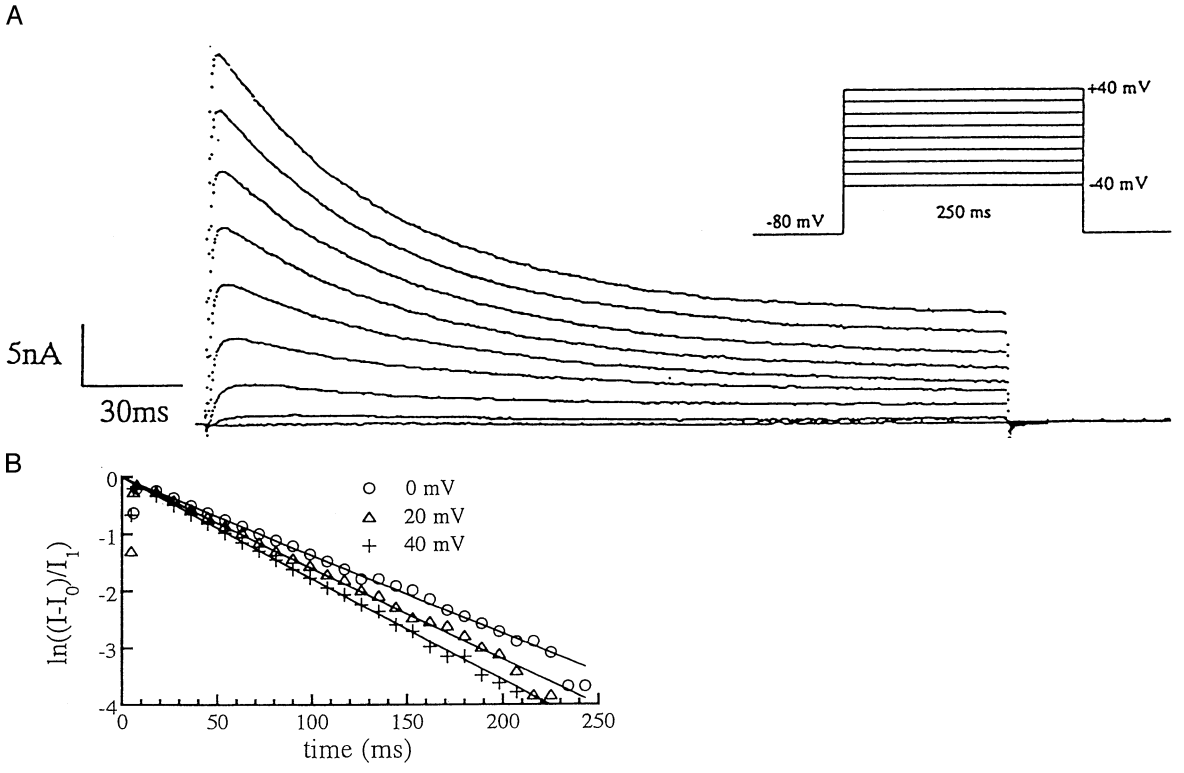

Fig. 2. The slow-inactivating current. (*A*) currents were recorded at 17°C from an axonless cell body a few hours after plating. Pulse protocol is as shown. (*B*) the inactivating phase of the current I could be fitted by the form $I = I_0 + I_1 e^{-t/\tau}$, where τ is the inactivation time constant. Representative points of $(I - I_0)/I_1$ are plotted for traces in *A* corresponding to 0 (○), 20 (Δ) and 40 mV (+) in logarithmic scale together with their corresponding exponential fit shown in solid lines. The inactivation time constants are 73.3, 64.1 and 55.6 msec for 0, 20, and 40 mV respectively.

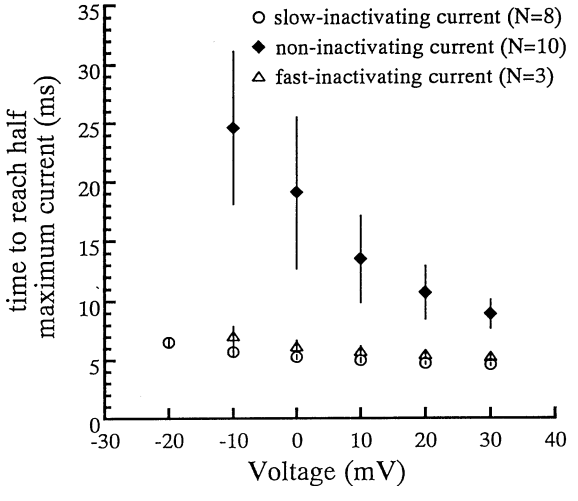

Fig. 3. Time to reach half maximum current vs. voltage. Plotted are mean values ± SD, obtained by averaging over *N* cells. Data shown are for the slow-inactivating current recorded from axonless cell bodies (○, $N = 8$), the noninactivating current comprising the only outward current recorded from some bulblike structures (◆, $N = 10$), the fast-inactivating current recorded from some bulblike structures (Δ, $N = 3$). Currents were recorded from GFL within 24 hr of plating at 17°C. The membrane potential was stepped from holding potential of −80 mV to the indicated voltages.

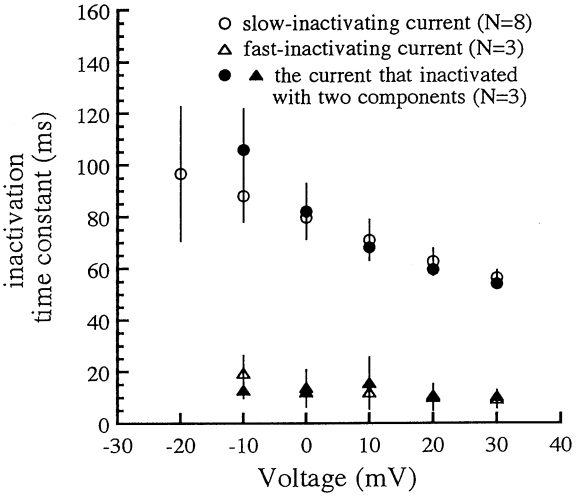

Fig. 4. Inactivation time constants *vs.* voltage. The currents were recorded in the same manner as that in Fig. 3. The inactivating phases of the currents were then fitted with one or two exponential functions. The time constants of these exponential functions are plotted. The mean values of the inactivation time constants, averaged over *N* cells, together with SD, are shown for the slow-inactivating current recorded from axonless cell bodies (○, $N = 8$), the fast-inactivating current recorded from some bulblike structures (Δ, $N = 3$) and the components that inactivated faster (▲) and more slowly (●) recorded from some axonless cell bodies that elicited two inactivating components ($N = 3$).

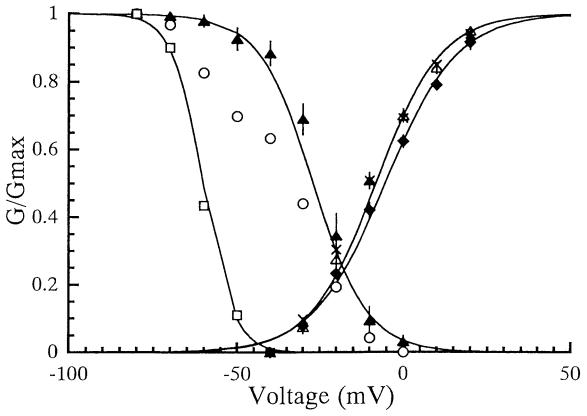

Fig. 5. Activation and inactivation of the potassium currents. Currents were recorded from different structures of GFL within 24 hr of plating at 17°C. The smooth curves are fit to the mean values by Boltzmann function of the form $G/G_{max} = 1/(1 + e^{(V-V1/2)/k})$, where V is the membrane potential, $V_{1/2}$ is the voltage at which the conductance reaches half maximum and k is the slope factor. The conductance was calculated using $G = I_{peak}/(V - E_k)$, where I_{peak} is the peak current corresponding to membrane potential V and E_k is the reversal potential. E_k are −54 and −50 mV for the slow-inactivating current and the noninactivating current respectively (*see* Fig. 6). Conductance as a function of voltage obtained for each cell was first fit to the Boltzmann function, normalized with the maximum conductance and finally averaged over N cells. The activation curve of the slow-inactivating current (Δ, $N = 11$) has a midpoint of −8.2 mV and a slope of −9.7 mV. The activation characteristics did not change when no calcium was included in the external solution (×). The activation curve of the noninactivating current (♦, $N = 3$) is slightly shifted to more positive voltages, with a midpoint of −5.5 mV and a slope of −10.7 mV. The steady-state inactivation was examined by stepping the potential to +20 mV after prepulses that last 1 sec with voltages ranging from −80 to +20 mV. About 20% of the maximum of the peak current was not inactivated and this amount was subsequently subtracted from the data. The steady-state inactivation of the slow-inactivating current (▲, $N = 5$) has a half-inactivation point of −26.9 mV and a slope of 8.1 mV. The inactivation of the current which inactivated with a faster and a slower component (○), recorded from an axonless cell body (*see* Fig. 11*A*), deviated from that of the slow-inactivating current at more negative voltages. The inactivation of the fast-inactivating component (□) could be fitted by a Boltzmann function with a midpoint of −60.2 mV and a slope of 4.6 mV.

ternal solution, unless otherwise noted, consisted of (in mM): 435 NaCl, 10 KCl, 10 $CaCl_2$, 50 $MgCl_2$, 5 glucose, 10 HEPES (pH 7.8). When a different external K^+ concentration was used, NaCl was used as an equimolar substitute to maintain the ionic strength.

The internal solution in all the experiments contained (in mM): 250 K-glutamate, 25 KF, 20 KCl, 400 sucrose, 10 Na_2-EGTA and 10 HEPES (pH 7.8). Patch pipettes used for recording from the axonless cell bodies had resistance 0.6–0.7 MΩ when filled with the internal solution. Patch pipettes with resistance of 0.8–0.9 MΩ were used when recording from the axonal bulbs and the bulblike structures.

Currents were recorded using Axopatch 200A (Axon Instruments). Through TL-1 DMA interface (Axon Instruments), stimulation, data acquisition and analysis were performed using pCLAMP software (Version 5.1, Axon Instruments). Liquid junction potential was compensated for prior to seal formation. Series resistance compensation was adjusted to 70–80%. Linear leakage was subtracted using the -P/4 procedure. Currents were filtered at 1 KHz. The holding potential was −80 mV in all the experiments.

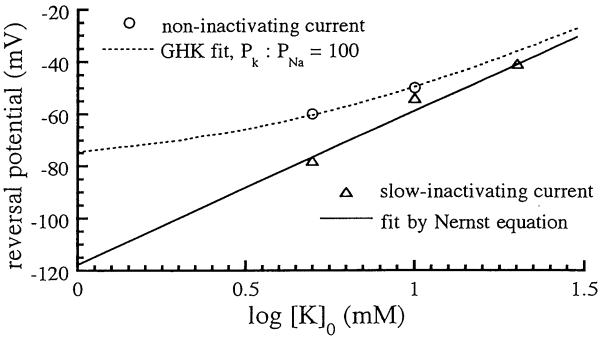

Fig. 6. Reversal potential as a function of the logarithm of the external potassium concentration ($[K]_0$). The reversal potential was measured as the potential corresponding to the zero tail current after the membrane was first depolarized from holding potential of −80 to +20 mV for 100 msec, followed by pulses of voltages between −90 and −20 mV. The values of the reversal potentials for the slow-inactivating current (Δ), and the noninactivating current that comprised the only outward current in some bulblike structures (○) are shown. The continuous line is a straight line fit with slope 25.0 mV, corresponding to 18°C following Nernst Equation. The dotted curve is a fit Goldman-Hodgkin-Katz equation with P_K:$P_{Na} = 100$.

Abbreviations

GFL, giant fiber lobe; 4-AP, 4-aminopyridine; 3,4-DAP, 3,4-diaminopyridine; TEA, tetraethylammonium; ASW, artificial sea water; DTX, dendrotoxin; CTX, charybdotoxin; TTX, tetrodotoxin

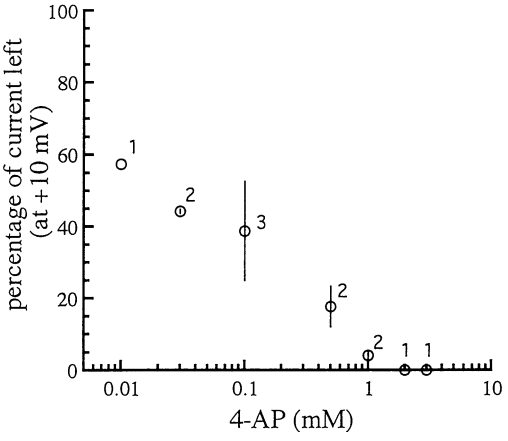

Fig. 7. Dose response to externally applied 4-AP. Currents were recorded from axonless cell bodies within 24 hr of plating at 17°C. The inactivating phases of the currents were comprised mainly of one exponential component (the slow-inactivating current). The dose response was measured as the percentage of peak current left after the application of 4-AP, at a membrane potential of +10 mV. Four-AP was added with bath application method. The number by each point indicates the number of cells over which the mean ± SD was obtained. The 4-AP concentration is in logarithmic scale.

Table 1. Currents elicited in different structures of the GFL within 24 hr of plating and the currents elicited by axonless cell bodies after being maintained in culture for over three days

		Potassium currents			Sodium current
		Slow-inactivating	Fast-inactivating	Noninactivating	
Within 24 hours of plating	Axonless cell body	all	some (~22%)	none	none
	Axonal bulb	all	some (~30%)	all	all
	Bulblike structure	some (~27%)	some (~18%)	all	all
In culture	Axonless cell body	all	some (~14%)	some (~86%)	some (~50%)

''all'' at ''slow-inactivating current'' and ''axonless cell body'' means that the slow-inactivating current was present in all the axonless cell bodies tested.

Results

Ionic Currents in Acutely Dissociated Structures of GFL

Slow-inactivating Potassium Current

The currents recorded from the acutely dissociated axonless cell bodies were comprised mainly of outward currents and the current composition did not change within 24 hr of plating. No detectable sodium currents were recorded, as was the case in acutely dissociated GFL cells of *Loligo opalescens* and *Lolliguncula brevis* [2, 8, 9]. Typical current traces are shown in Fig. 2A. The currents started to activate between −40 and −30 mV and rose rapidly, reaching half-maximum at 4.6 ± 0.1 msec (+30 mV) to 6.5 ± 0.4 msec (−20 mV) ($N = 8$, circles in Fig. 3), weakly depending on the voltage. The currents inactivated strongly, leaving 20~30% of their peak values at the end of 250 msec depolarization. In Fig. 2*B*, representative points from the traces corresponding to 0, 20 and 40 mV in Fig. 2*A* are plotted in logarithmic scale together with their corresponding exponential fit shown in straight lines. As shown in Fig. 2*B*, the falling phases could be fitted well by single exponential forms with offset of the size of 20–30% of the peak values. The inactivation time constants, ranged from 56.4 ± 2.9 msec (+30 mV) to 96.7 ± 26.0 msec (−20 mV) ($N = 8$, open circles in Fig. 4), increasing with more negative voltages.

Peak conductance (marked as open triangles) and steady-state inactivation (marked as filled triangles) as functions of voltage are shown in Fig. 5. The peak conductance curve could be fitted by a Boltzmann distribution with half-activation at −8.2 mV and a slope of −9.7 mV. The steady-state inactivation curve could also be approximated by a Boltzmann distribution having a midpoint of −26.9 mV and a slope of 8.1 mV.

The reversal potential increased as the external K^+ concentration was increased, following Nernst equation as plotted in Fig. 6 (triangles). The reversal potential was determined as the potential corresponding to zero tail current when pulses with voltages between −90 and −20 mV were applied, after the membrane was first depolarized from holding potential of −80 to +20 mV for 100 msec.

The outward current was sensitive to blockage by externally applied 4-AP. A dose-sensitive curve is shown in Fig. 7. 4-AP (2 mM) totally blocked the outward current, leaving a small inward current having characteristics similar to the calcium currents found by Llano and Bookman in *Loligo pealei* [19]. The selective permeability to potassium ions and the sensitivity to 4-AP established the outward current to be potassium current.

External application of CTX (Alomone Labs, Israel) up to 300 nM did not block the currents significantly. Removal of the external calcium ions did not change the outward current characteristics. Normalized peak conductance *vs.* voltage, when the calcium ion was not included in the external solution, is shown in Fig. 5 (marked as ''x''). These results show that the outward potassium current was not calcium-dependent. External application of αDTX (Alomone Labs, Israel) up to 300 nM did not block the currents significantly either.

The potassium current elicited by the axonless cell bodies resembled that found in the cell bodies of the GFL of *L. pealei* [19] in its activation and inactivation kinetics, but differed in its 4-AP sensitivity. Compared with another kind of inactivating potassium current that will be described later, this current had slower inactivation time constants and is referred to as the slow-inactivating potassium current.

This slow-inactivating potassium current also was elicited in all the axonal bulbs and about 27% of the bulblike structures, as illustrated in Table 1.

Noninactivating Potassium Current and Sodium Current

Obvious sodium currents were present in the acutely dissociated bulblike structures, in contrast to the case in the cell bodies. The sodium currents were totally blocked by 100 nM TTX (Molecular Probes). Current traces re-

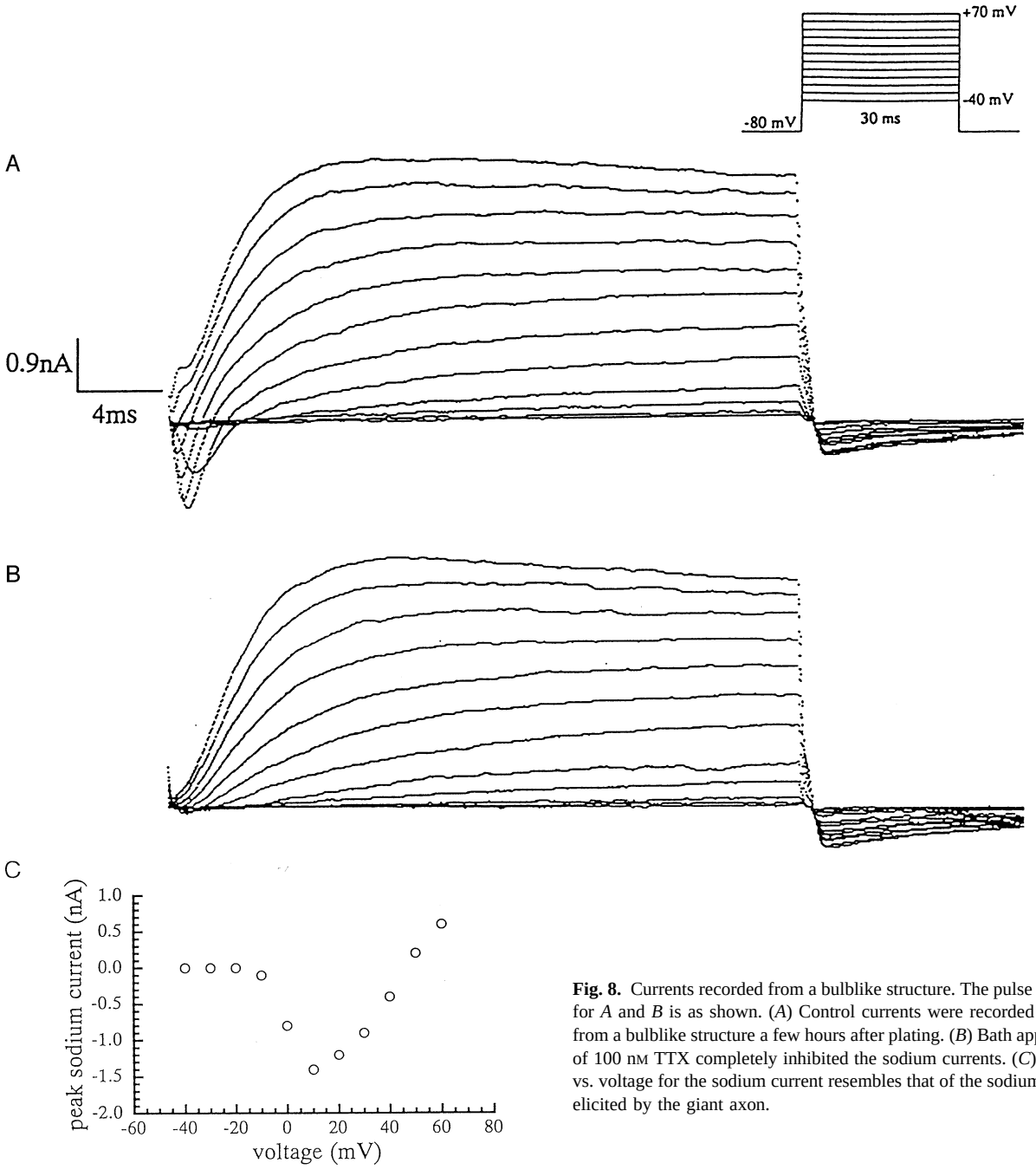

Fig. 8. Currents recorded from a bulblike structure. The pulse protocol for *A* and *B* is as shown. (*A*) Control currents were recorded at 17°C from a bulblike structure a few hours after plating. (*B*) Bath application of 100 nM TTX completely inhibited the sodium currents. (*C*) Current vs. voltage for the sodium current resembles that of the sodium current elicited by the giant axon.

corded from a bulblike structure before and after application of 100 nM TTX are shown in Fig. 8*A* and *B* respectively. The current-voltage relation of the sodium current is shown in Fig. 8*C*. The sodium current is similar to that normally elicited by the giant axon. Axonal bulbs also elicited sodium current with similar characteristics (*data not shown, see* Table 1).

The currents shown in Fig. 9*A* were recorded from a bulblike structure with 100 nM TTX included in the bath solution to block the sodium currents. The outward current started to activate between −30 and −20 mV. It rose more slowly than the slow-inactivating currents. The time to reach half maximum current for this current is shown in Fig. 3 (marked as diamonds). Little inactivation was observed over 250 msec. To distinguish it from the transient potassium current, we will refer to it as the nonactivating current.

Normalized peak conductance of the noninactivating current as a function of voltage is shown in Fig. 5 (marked as diamonds). It can be fitted with a Boltzmann

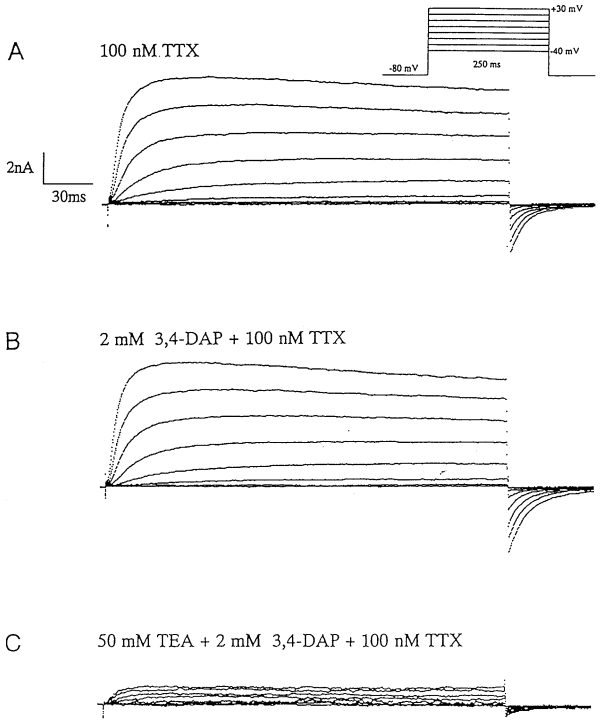

Fig. 9. The noninactivating current comprising the only outward current in a bulblike structure. The currents were recorded from a bulblike structure a few hours after plating at 17°C. The bath solution contained 100 nM TTX to inhibit the sodium current. The pulse protocol is as shown. (*A*) The outward current hardly inactivated over 250 msec. (*B*) Bath application of 2 mM 3,4-DAP did not affect the currents. (*C*) Bath application of 50 mM TEA inhibited about 85% of the current. When applied alone, 50 mM TEA had the same effect (*data not shown*).

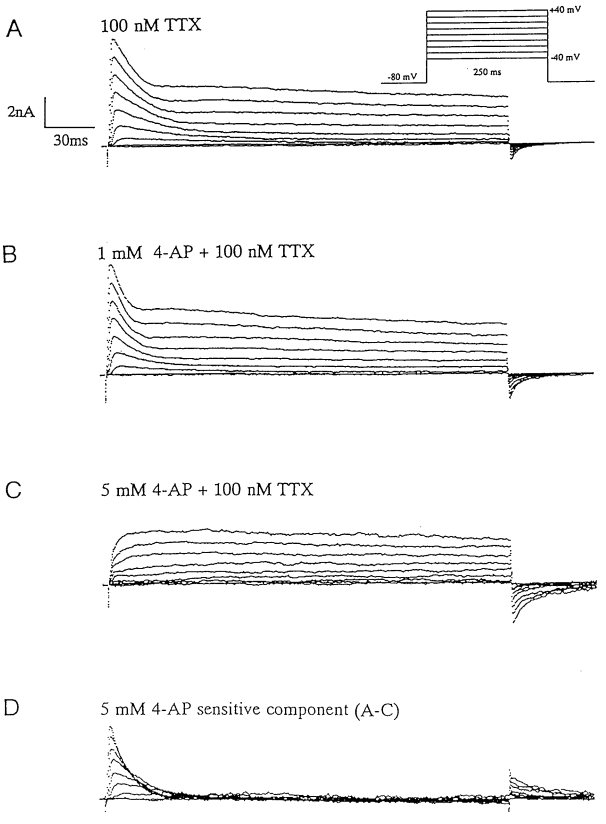

Fig. 10. The fast-inactivating current coexisting with the noninactivating current in a bulblike structure a few hours after plating at 17°C. The pulse protocol for *A–D* is as shown. TTX (100 nM) was included in the bath solution to eliminate the sodium current. (*A*) total outward currents. (*B*) Bath application of 1 mM 4-AP left the currents unaffected. (*C*) Bath application of 5 mM 4-AP completely inhibited the fast-inactivating component, leaving only the noninactivating component. (*D*) Subtraction of the corresponding traces of *C* from *A* gives fast-inactivating, totally inactivating current traces.

function with midpoint at −5.5 mV and a slope of −10.7 mV. The activation curve is slightly shifted to more positive voltages compared with that of the slow-inactivating current.

The reversal potential, shown in Fig. 6 (circles) was determined in the same manner as that used for the slow-inactivating current. It is more positive than that predicted by the Nernst equation especially at low external potassium concentration (*see* Fig. 6), indicating that the channels are also slightly permeable to the sodium ions, with $P_K{:}P_{\mathrm{Na}} = 100$.

Two millimeters of 3,4-DAP (*see* Fig. 9*B*) or 4-AP (*data not shown*) applied externally did not affect the noninactivating current. Externally applied 50 mM TEA inhibited 85% of this noninactivating current (*see* Fig. 9*C*). The dependence of the reversal potential on the external potassium concentration and the sensitivity to TEA established this noninactivating current to be potassium currents. Similar currents could also be observed from axonal bulbs, after the inhibition of the sodium current by 100 nM TTX and the inhibition by 1 mM 4-AP of the current component that resembled the slow-inactivating current (*see* Table 1).

Fast-inactivating Potassium Current

Fast-inactivating Potassium Current in Some Acutely Dissociated Bulblike Structures. Some bulblike structures elicited a combination of the sodium current and the noninactivating potassium current as shown before. In addition to these currents, a current component that resembled the slow-inactivating current was coelicited by some bulblike structures, as is the case for the axonal bulbs. In other bulblike structures, aside from the sodium current and the 4-AP insensitive noninactivating outward current, there was also a fast-inactivating outward current. Such a case is shown in Fig. 10*A*. The external solution contained 100 nM TTX to inhibit the sodium current. External application of 1 mM 4-AP did not affect the currents (Fig. 10*B*), while 5 mM 4-AP inhibited all the fast-inactivating component, leaving only the noninactivating component (Fig. 10*C*). Subtraction of the traces in Fig. 10*C* from those in Fig. 10*A*,

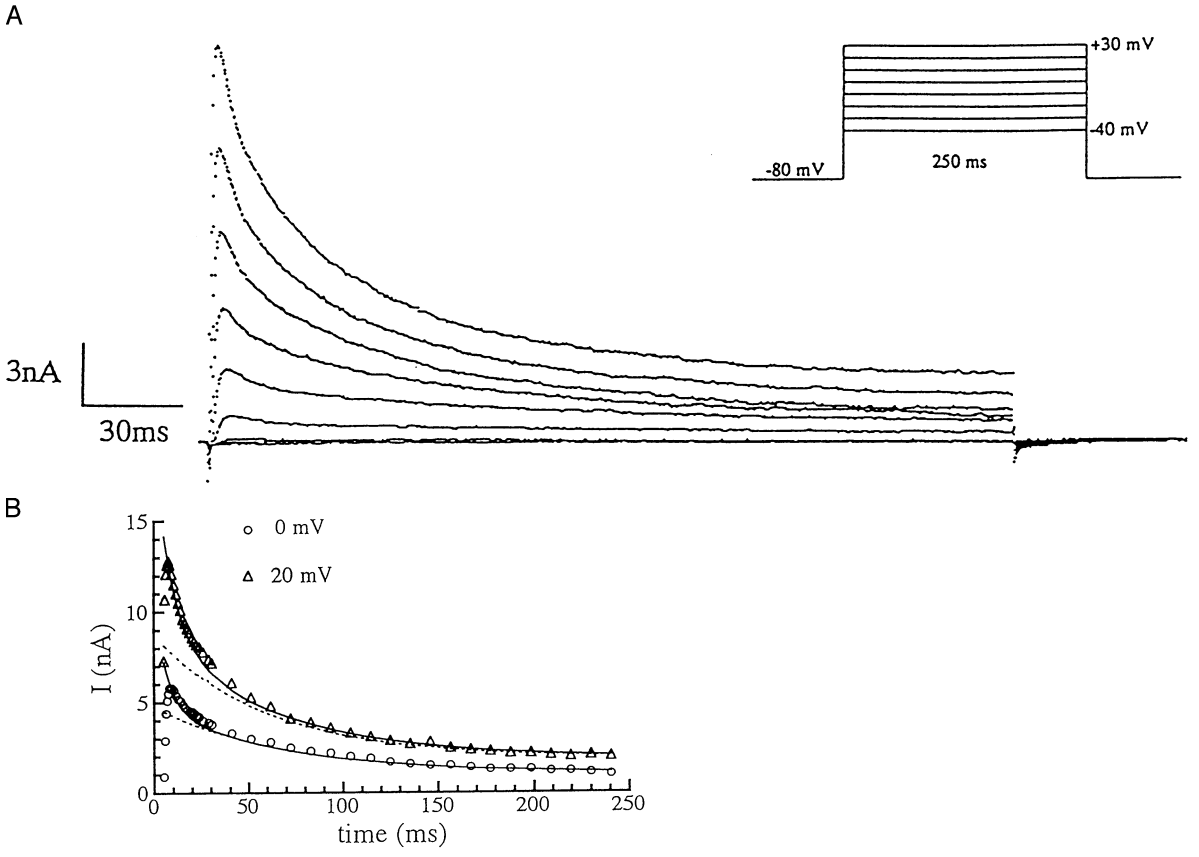

Fig. 11. Current traces eliciting outward currents with inactivating phases fitted by two exponential functions. (*A*) Currents were recorded at 17°C from an axonless cell body a few hours after plating. The pulse protocol is as shown. (*B*) Representative points from traces in *A* corresponding to 0 (○) and 20 mV (Δ) are shown together with their corresponding fit by two exponential functions shown in solid curves. Fit to the late time inactivating phase by one exponential function in also shown in dotted curve. The inactivation time constants, in msec, of the faster and the slower components are 6.5 and 68.3; 9.8 and 65.0 respectively for 0 mV, 20 mV.

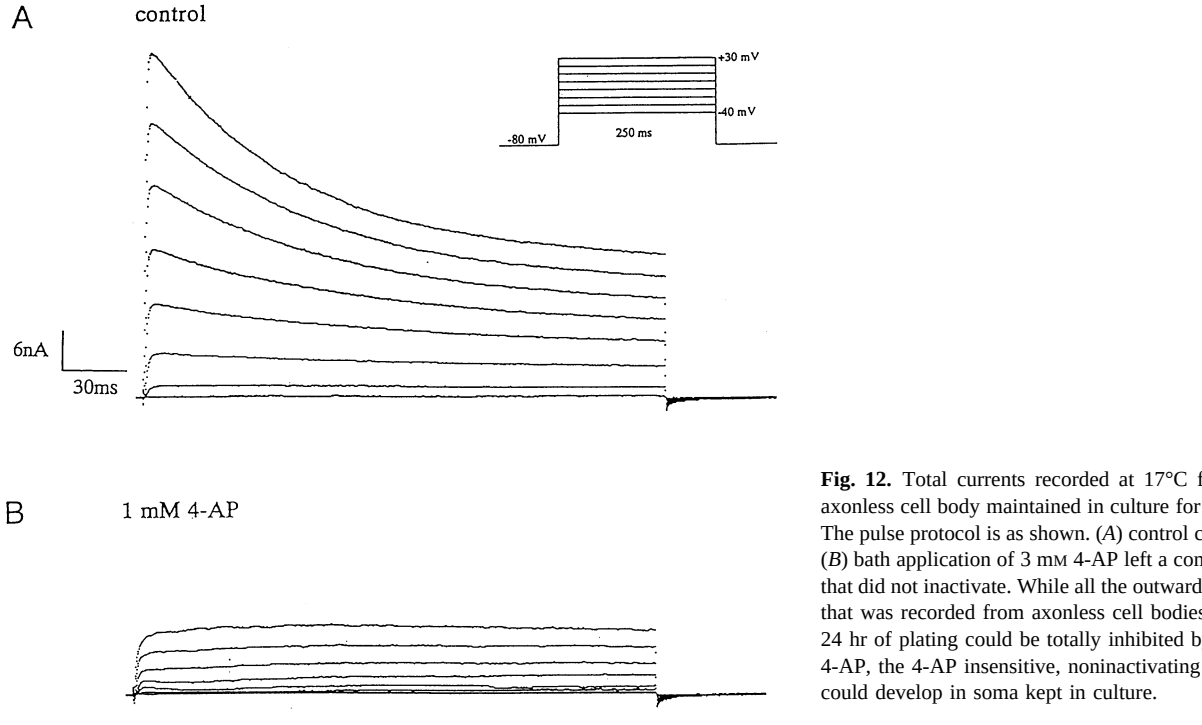

Fig. 12. Total currents recorded at 17°C from an axonless cell body maintained in culture for 9 days. The pulse protocol is as shown. (*A*) control currents. (*B*) bath application of 3 mM 4-AP left a component that did not inactivate. While all the outward current that was recorded from axonless cell bodies within 24 hr of plating could be totally inhibited by 3 mM 4-AP, the 4-AP insensitive, noninactivating current could develop in soma kept in culture.

Table 2. Comparison of the kinetic properties and 4-AP sensitivity of the three potassium currents from GFL and the delayed rectifying potassium current from the giant axon

		Kinetic properties				4-AP needed for total current blockage
		Time to reach half maximum current (msec)	Inactivation time constants (msec)	Half activation (mV)	Half inactivation (mV)	
Potassium currents from GFL	Slow-inactivating current	4.6 ± 0.1 (30 mV)/ 5.7 ± 0.3 (−10 mV) (N = 8)	56.4 ± 2.9 (30 mV)/ 96.7 ± 26 (20 mV) (N = 8)	−8.2	−26.9	2 mM
	Fast inactivating current	5.3 ± 0.2 (30 mV)/ 7.1 ± 0.8 (−10 mV) (N = 3)	9.4 ± 3.5 (30 mV)/ 19.4 ± 6.9 (−20 mV) (N = 3)	ND	−60.2	5 mM
	Noninactivating current	8.9 ± 1.2 (30 mV)/ 24.6 ± 6.5 (−10 mV) (N = 10)		−5.5		not sensitive up to 5 mM
Delayed rectifying potassium current from giant axon[a]		submilliseconds[b]	770 msec and 4.15 sec [3]	0[b]	−55 [3]	100 μM[b]

ND, not determined.

[a] Kinetic numbers were corrected for temperature at 17°C.

[b] These numbers were obtained from the giant axon of *Loligo bleekeri* by M. Ichikawa (*personal communication*).

as shown in Fig. 10*D*, gives fast-inactivating, totally inactivating currents. The time to reach half maximum of these fast-inactivating current was close to that of the slow-inactivating current, being 5.3 ± 0.2 msec (+30 mV) to 7.1 ± 0.8 msec (−10 mV) (N = 2, triangles in Fig. 3). The inactivation time constants of these fast-inactivating components were in the range of 9.4 ± 3.5 msec (+30 mV) to 19.4 ± 6.9 msec (−10 mV) (N = 4, open triangles in Fig. 4). Compared with the slow-inactivating current elicited by the axonless cell bodies, the fast-inactivating current has smaller inactivation time constants and was less sensitive to inhibition by 4-AP.

Fast-inactivating Potassium Current in Some Acutely Dissociated Axonless Cell Bodies. In some axonless cell bodies, current traces like those shown in Fig. 11*A* were recorded. The dominant component of the falling phase was like the slow-inactivating current. There was an additional inactivating phase that inactivated faster with time constants in the range of 10.4 ± 1.5 (−10 mV) to 12.9 ± 3.1 msec (+30 mV) (N = 3, filled triangles in Fig. 4). Figure 11*B* shows representative points from traces corresponding to 0, and 20 mV in Fig. 11*A* together with fit by superposition of two exponential functions shown in solid curves. Fit of the slower component by one exponential function is shown in dotted curve. While the long-time behavior could be well approximated by one exponential function, the short-time behavior needs an additional exponential function with faster inactivation time constant. The inactivation time constants of the component that inactivated more slowly were 54.1 ± 0.5 msec (+30 mV) to 105.9 ± 15.9 msec (−10 mV) (N = 3, filled circles in Fig. 4), larger for more negative voltages. These values agreed with those of the slow-inactivating current that was elicited as the only outward current component in the axonless cell bodies described previously (*see* Fig. 4). The inactivation time constants of the component that inactivated faster did not depend on the voltage significantly and their values agreed with those of the fast-inactivating current elicited by the bulblike structures (*see* Fig. 4).

The component that inactivated more slowly could be mostly inhibited by 1 mM 4-AP like the slow-inactivating current (data not shown). The component that inactivated faster was less sensitive to 4-AP, similar to the fast-inactivating current in some bulblike structures. The slower and the faster components will also be referred to respectively as the slow- and the fast-inactivating current.

The steady-state inactivation curve is shown in Fig. 5 (open circles) for the same cell that exhibited current traces in Fig. 11*A*. The curve deviates from that of the slow-inactivating current at lower voltages, indicating that the inactivation curve of the fast-inactivating current is shifted to more negative voltages. The inactivation of the fast-inactivating component can be obtained by subtracting the inactivation of the slow-inactivating component (which is about 72.1% in this case) from the total inactivation. The result is shown as empty squares. It can be fitted well by a Boltzmann distribution with half inactivation at −60.2 mV and a slope factor of 4.6 mV.

Development of Ionic Currents in Axonless Cell Bodies Maintained in Culture

The current composition did not vary in some cells up to day 9 in culture, while other cells exhibited a range of

Table 3. Kinetic and pharmacological properties of the D current (I_D) and the *A* current (I_A) that coexist in rat hippocampal neurons [30], embryonic rat hippocampal neurons [7], embryonic mouse hippocampal neurons [31] and GFL

	Kinetic properties									
	Rising kinetics		Half activation voltage(mV)		Half inactivation voltage(mV)		Inactivation time constants		Voltage dependence of inactivation time constants	
	I_D	I_A	I_D	I_A	I_D	I_A	I_D	I_A	I_D	I_A
Rat hippocampal neurons	rapid	rapid	NA	NA	-88	-60	<seconds	<50msec	NA	NA
Embryonic rat hippocampal neurons	fast	fast	~5[b]	-19	-61	-81	500msec and 3.5sec	~10msec	not dependent	slightly more rapid at more positive voltages
Embryonic mouse hippocampal neurons	fast[a]	fast[a]	0	-17	-22	-81	200msec(+40mV)~ 7sec(-40mV) and slower component	20~25 msec	more rapid at more positive voltages	not dependent
GFL	4.6~ 6.5 msec	5.3~ 7.1 msec	-8.2	NA	-27	-60	56.4(+30mV)~ 96.7msec(-20mV) and slower component	9~19 msec	more rapid at more positive voltages	not dependent

The slow transient current in embryonic rat hippocampal neurons categorized as I_D here is denoted as $I_{T,\text{slow}}$ in [7]. The slow- and fast-decaying currents in GFL are denoted as I_D and I_A respectively in this table.

[a] determined from the current traces in [31].

[b] determined from Fig. 3 in [7]. The activation curve for I_D was not described by the Boltzmann function. The half activation voltage is determined as the voltage at which the conductance reaches half of that at +30 mV.

[c] NA not available.

behaviors. The difference did not seem to stem from the preparation since cells in the same culture dish could exhibit different behaviors.

In some axonless cell bodies, sodium currents were recorded after day 3 in culture (*data not shown*) as reported in cultured GFL cell bodies of *L. opalescens* and *L. brevis* [2, 8, 9]. In the case of the outward potassium current, the 4-AP insensitive, noninactivating current also developed in some axonless cell bodies (*see* Fig. 12*A* and *B*).

The appearance of the sodium current and the noninactivating potassium current in the axonless cell bodies does not seem to be caused by contamination from possible retraction of the axonal bulbs into the soma which could happen in the first few days in culture [9]. These new currents in soma in later days have larger amplitudes than those in bulbs in the first 0 to 2 days. Brismar and Gilly [2] cultured the dissociated cells from GFL of *L. opalescens* and *L. brevis* in actinomycin, an mRNA synthesis inhibitor, and found that the sodium currents, which first appeared from probable insertion of the already synthesized channels, disappeared on the time scale of 1.2 days. The lifetime of the sodium channels was estimated to be at most 1.2 days, taking into account that the mRNA also has a lifetime. If this is also the case for the sodium currents and the potassium currents in the GFL of *L. bleekeri,* then the new currents recorded in cells kept in culture for over 8 days are more likely to have come from insertion of the channels newly synthesized by the cells maintained in culture.

Conclusions and Discussion

Ionic currents through the voltage-dependent ion channels were recognized by Hodgkin and Huxley to play a central role in the electrical excitability of the membrane of squid giant axon [13, 14, 15]. These currents in squid giant axon have since been extensively characterized (*see* [12]). The sodium current functions to generate the rapid rising phase of the action potential. The potassium current which is activated with a delay upon membrane depolarization flows through so-named delayed rectifying potassium channels. This delayed rectifying current has been found to be ubiquitously distributed and responsible for repolarizing the membrane (*see* [12]). Although the potassium current in Hodgkin and Huxley's description does not inactivate, later studies with prolonged depolarizing pulses revealed slow inactivation with two time constants on the order of seconds and tens of seconds respectively (*see* [3]). This current is sensitive to the blockage by external 4-AP and 3,4-DAP and internal TEA, but not sensitive to blockage by up to 100 mM TEA applied externally (for review, *see* [28]).

Table 3. (*Continued*)

Pharmacological properties			
Amount of 4-AP for complete blockage		DTX sensitivity	
I_D	I_A	I_D	I_A
30μM	1~5mM	NA	NA
depressed by 50μM, cannot be totally blocked by 2mM	>10mM	NA	insensitive (600 nM)
100μM	2~3mM	1μM	>1~2μM
2mM	5 mM	insensitive (300 nM)	NA[c]

GFL of *L. pealei* was cultured successfully by Llano and Bookman [19]. The currents recorded from acutely dissociated cells were comprised mostly of outward potassium current. When a few tens of milliseconds of depolarization pulses were applied, this potassium current resembled that in the giant axon in its voltage dependence of the activation and the time to reach half maximum current. Longer depolarization pulses lasting 250 msec revealed strong inactivation, leaving 35–40% of the peak values at the end of the pulses. The inactivation time constants at 10–12°C were 80–100 msec. These potassium currents were insensitive to 4-AP or TEA applied externally and could be blocked by internally applied TEA. The inward current, sometimes a small fraction of which was sodium current, was mainly carried by calcium ions.

It has been known that while the giant axon membrane has a high density of voltage-dependent sodium channels which contributes to its electrical excitability, the cell bodies of the giant axon in GFL, where probably most of the functional sodium channels of the giant axon are synthesized, is not excitable *in vivo* [25]. Ionic currents, in particular the sodium currents have been studied in cultured GFL of *L. opalescens* and *L. brevis* [2, 8, 9]. The synthesis and transportation of the sodium channels have been examined. These studies showed that while sodium channels were preferentially expressed in the axonal membrane in culture, sodium currents indistinguishable from those in giant axon did develop in somata that were kept in culture. Cytoskeleton seems to be involved in the transportation of the newly synthesized sodium channels to the somatic membrane [2]. These results indicate that GFL neurons maintained in primary culture are capable of synthesizing and inserting functional sodium channels into the somatic and the axonal membrane, with a preference for the axonal membrane.

We reported here the identification and isolation of three kinds of biophysically and pharmacologically distinct voltage-dependent potassium currents from acutely dissociated GFL. The main kinetic and pharmacological properties of these three potassium currents are compared with the delayed rectifying potassium current from the giant axon in Table 2.

The two inactivating potassium currents identified here had characteristics that are usually associated with A currents [5, 11, 26]. These two currents activated and inactivated faster and were more sensitive to 4-AP, compared with the noninactivating potassium current which resembled the delayed rectifying potassium current in squid giant axon [13, 14, 15]. The currents that have been generally categorized as A currents show a wide range of diversity in their inactivation time constants and their 4-AP sensitivity (for review, *see* [1, 6, 28]). Recently, currents with slower inactivation and enhanced 4-AP sensitivity, which had been previously categorized as A-current variants, have been identified in several types of cells to coexist with A currents. These currents are sometimes called D currents (*see,* [7, 30, 31]). The voltage dependence of the inactivation time constants of the slow- and the fast-inactivating current in GFL is respectively similar to that of the D and A current in cultured embryonic mouse hippocampal neurons [31], while different from that of the slower and the faster component in cultured embryonic rat hippocampal neurons [7]. In GFL, the inactivation curve of the A current is shifted to more negative voltage compared with that of the D current, as is also the case in cultured embryonic mouse hippocampal neurons [31] and cultured embryonic rat neurons [7]. By comparison, in rat hippocampal neurons the half-inactivation of the A current was about 20 mV more positive than that of the D current [30]. The differential sensitivity to 4-AP of the slow- and the fast-inactivating currents in GFL was comparable to that in the rat [30] and the embryonic mouse [31] hippocampal neurons. While the D current in embryonic mouse hippocampal neurons was preferentially blocked by 1 mM DTX [31], up to 300 nM αDTX did not have significant effect on the slow-inactivating component in GFL, nor did DTX up to 600 nM on the slower component in embryonic rat hippocampal neurons [7]. The slow- and the fast-inactivating currents have distinct properties and are D- and A-currentlike respectively. A detailed comparison of these properties is presented in Table 3.

Although the noninactivating current resembled the delayed rectifying potassium current in squid giant axon [13, 14, 15] in terms of its inactivation properties, their detailed kinetic and pharmacological properties were different. Both currents rise upon membrane depolarization in a voltage-dependent manner, more slowly with more

negative voltages. The noninactivating current here is in general slower, reaching half-maximum at 8.9 ± 1.2 msec (+30 mV) to 24.6 ± 6.5 msec (−10 mV) (N = 10, diamonds in Fig. 3) instead of submilliseconds in the case of the delayed rectifying current in the giant axon. Externally applied 2 mM 3,4-DAP (*see* Fig. 9*B*) or 4-AP (*data not shown*) left the noninactivating current in GFL unaffected, while the delayed rectifying current in the giant axon can be completely inhibited under the same conditions. While up to 100 mM TEA applied externally does not block the delayed rectifying current in the giant axon, about 85% of this noninactivating current in GFL could be inhibited with 50 mM TEA when applied externally.

The offset in the exponential function to fit the inactivating phase of the slow-inactivating current does not seem to come from a noninactivating current, at least not the kind that is similar to that elicited by the axonal bulbs or the bulblike structures. This is because the external application of 2 mM 4-AP totally inhibited the slow-inactivating current, including this offset component, while the noninactivating current was not sensitive to external application of up to 5 mM 4-AP. Examination of the currents recorded with longer depolarization (*data not shown*) shows that the offset at the end of 1 sec further decreases 20–35% compared with that at 250 msec, indicating the probable presence of another slower component with time constants on the order of seconds. D currents in embryonic rat hippocampal neurons also inactivate with two time constants, in the order of 500 msec and 3.4 sec respectively [7]. Such an additional slower component in the D current was also suggested in the embryonic mouse hippocampal neurons [31].

The three potassium currents together with the sodium current appeared in different combinations in the axonless cell bodies, the axonal bulbs and the bulblike structures upon their dissociation. The current composition, as illustrated in Table 1, did not change within 24 hr of plating. In axonless cell bodies, the dominant current was a slow-inactivating potassium current. Aside from the sodium current, a noninactivating outward current was found to be the only potassium current in some bulblike structures. Some bulblike structures elicited a fast-inactivating potassium current in addition to the noninactivating potassium current and the sodium current. Similar fast-inactivating current could also be recorded, together with the dominant slow-inactivating current, from some axonless cell bodies, some axonal bulbs and some bulblike structures.

The axonless cell bodies maintained in culture for over three days could elicit currents that were not elicited upon dissociation, specifically, the sodium current and the noninactivating, 4-AP insensitive potassium current. The current composition in axonless cell bodies maintained in culture for over 3 days is also illustrated in Table 1.

Our results show that a selective combination of different channel functions was expressed in each of the axonless cell body, axonal bulb and bulblike structure in GFL and that this selectivity could vary in time. The potassium currents of the types that were recorded upon dissociation were also present in cells maintained in culture for up to 9 days. Moreover, the types of currents that were present in axonal membrane and not present in soma upon dissociation could develop in soma maintained in culture. These facts suggest that the cells maintained in culture are capable of synthesizing all types of currents observed in GFL and are probably the main source of the corresponding channels on the membrane of the axonal bulbs, the bulblike structures and the giant axon. While a combination of all the currents can be recorded from membrane of the axonal bulbs which reside in between the soma and the giant axon, the giant axon and its soma elicit different currents. Currents similar to the sodium and delayed rectifying potassium current of the giant axon are also elicited by the axonal membrane of the axonal bulbs and bulblike structures, while the somatic membrane does not elicit these currents. The slow-inactivating potassium current, which is the main current expressed on the somatic membrane, is also elicited in the proximal axonal membrane (axonal bulbs), while not in giant axon.

When GFL is maintained in culture, the giant axon, which serves *in vivo* as the destination of the newly synthesized proteins, is absent. As a result, while maintained in culture, the somata start to express some of the channel functions that are not expressed immediately upon dissociation. A similar situation has been reported for the sodium channels in cultured GFL of *L. opalescens* [9]. The axonal bulb has well-defined morphology and can be separated from its soma without disrupting its functions. Its properties can be recorded separately along with those of its soma [9]. GFL together with the giant axon provide an advantageous system for studying channel synthesis and distribution in the somatic, the proximal (the axonal bulb) and the distal (the giant axon) axonal membrane.

The authors are indebted to Professor Michael Barish for stimulating discussion. The authors also thank Professor M. Ichikawa and Dr. Xue-Song Zhang for helpful discussion. YH wishes to thank Professor R. Bookman and Professor W. Gilly for inspiring discussion and opportunities of visiting their labs while the GFL neurons were being prepared and cultured. WSDG acknowledges a NSF-administered Science and Technology Agency (Japan) postdoctoral fellowship and the hospitality of the Electrotechnical Laboratory where this research was performed.

References

1. Barish, M. 1994. Modulation of the electrical differentiation of neurons by interactions with glia and other non-neuronal cells. *Neurobiol. Pers. discussion* (*in press*)

2. Brismar, T., Gilly, W.F. 1987. Synthesis of sodium channels in the cell bodies of squid giant axons. *Proc. Natl. Acad. Sci. USA* **84:**1459–1463
3. Chabala, L.D. 1984. The kinetics of recovery and development of potassium channel inactivation in perfused squid (*Loligo pealei*) giant axon. *J. Physiol.* **356:**193–220
4. Christie, M.J., North, R.A., Osborne, P.B., Douglass, J., Adelman, J.P. 1990. Heteropolymeric potassium channels expressed in *Xenopus* oocytes from cloned subunits. *Neuron* **4:**405–411
5. Connor, J.A., Stevens, C.F. 1971. Voltage clamp studies of a transient outward membrane current in gastropod neural somata. *J. Physiol.* **213:**21–30
6. Dolly, J.O. 1988. Potassium channels—what can the protein chemistry contribute? *TINS* **11:**186–188
7. Ficker, E., Heinemann, U. 1992. Slow and fast transient potassium currents in cultured rat hippocampal cells. *J. Physiol.* **445:**431–455
8. Gilly, W.F., Brismar, T. 1989. Properties of appropriately and inappropriately expressed sodium channels in squid giant axon and its somata. *J. Neurosci.* **9**(4):1362–1374
9. Gilly, W.F., Lucero, M.T., Horrigan, F.T. 1990. Control of the spatial distribution of sodium channels in giant fiber lobe neurons of the squid. *Neuron* **5:**663–674
10. Griggs, W.-S.D., Hanyu, Y., Matsumoto, G. 1994. Selective expression of three distinct potassium channel activities in giant fiber lobe of squid. *Soc. Neuroscience* **20:** 1522*A (Abstr.)*
11. Hagiwara, S., Kusano, K., Saito, N. 1961. Membrane changes in *Onchidium* nerve cell in potassium-rich media. *J. Physiol.* **155:**470–489
12. Hille, B. 1992. Ionic Channels in Excitable Membranes. Sinauer, Sunderland, MA
13. Hodgkin, A.L., Huxley, A.F. 1952. Currents carried by sodium and potassium ions through the membrane of the giant axon of *Loligo. J. Physiol.* **116:**449–472
14. Hodgkin, A.L., Huxley, A.F. 1952. The components of membrane conductance in the giant axon of *Loligo. J. Physiol.* **116:**473–496
15. Hodgkin, A.L., Huxley, A.F. 1952. A quantitative description of membrane current and its application to conductance and excitation in nerve. *J. Physiol.* **117:**500–544
16. Honoré, E., Attali, B., Romey, G., Lesage, F., Barhanin, J., Lazdunski, M. 1992. Different types of K^+ channel current are generated by different levels of a single mRNA. *EMBO J.* **11:**2465–2471
17. Isacoff, E.Y., Jan, Y.N., Jan, L.Y. 1990. Evidence for the formation of heteromultimeric potassium channels in *Xenopus* oocytes. *Nature* **345:**530–534
18. Li, M., Jan, Y.N., Jan, L.Y. 1992. Specification of subunit assembly by the hydrophilic amino-terminal domain of the Shaker potassium channel. *Science* **257:**1225–1230
19. Llano, I., Bookman, R.J. 1986. Ionic conductances of squid giant fiber lobe neurons. *J. Gen. Physiol.* **88:**543–569
20. Matsumoto, G., Murofushi, H., Endo, S., Kobayashi, T., Sakai, H. 1982. Tyrosinated-tubulin necessary for maintenance of membrane excitability in squid giant axon, *In:* Structure and Function and Excitable Cells. Plenum, New York
21. Matsumoto, G., Murofushi, H., Sakai, H. 1980. The effect of reagents affecting microtubules and microfilaments on the excitation of the squid giant axon measured by the voltage-clamp method. *Biomed. Res.* **1:**355–358
22. Matsumoto, G., Sakai, H. 1979. Microtubules inside the plasma membrane of squid giant axons and their possible physiological functions. *J. Membrane Biol.* **50:**1–14
23. Matsumoto, G., Sakai, H. 1979. Restoration of membrane excitability of squid giant axons by reagents activating tyrosine-tubulin ligase. *J. Membrane Biol.* **50:**14–22
24. McCormack, K., Lin, J.W., Iverson, L.E., Rudy, B. 1990. *Shaker* K^+ channel subunits form heteromultimeric channels with novel functional properties. *Biochem. Biophys. Res. Commun.* **171:**1362–1371
25. Miledi, R. 1967. Spontaneous synaptic potentials and quantal release of transmitter in the stellate ganglion of the squid. *J. Physiol.* **192:**379–406
26. Neher, E. 1971. Two transient current components during voltage clamp in snail neurons. *J. Gen. Physiol.* **61:**385–399
27. Pongs, O. 1992. Molecular biology of voltage-dependent potassium channels. *Physiol. Rev.* **72:**S69–S88
28. Rudy, B. 1988. Diversity and ubiquity of K channels. *Neuroscience* **25:**729–749
29. Ruppersberg, J.P., Schroter, B., Sakkman, M., Stocker, S., Sewing, S., Pongs, O. 1990. Heteromultimeric channels formed by rat brain potassium-channel proteins. *Nature* **352:**711–714
30. Storm, J.F. 1988. Temporal integration by a slowly inactivating K^+ current in hippocampal neurons. *Nature* **336:**3379–381
31. Wu, R.-L., Barish, M.E. 1992. Two pharmachologically and kinetically distinct transient potassium currents in cultured mouse hippocampal neurons. *J. Neurosci.* **12:**2235–2246